Supramolecular Photocatalyst for the Reduction of Au(III) to Au(I) and High-Turnover Generation of Gold Nanocrystals

Cédric Mongin, Isabelle Pianet, Gediminas Jonusauskas, Dario M. Bassani, Brigitte Bibal

Supramolecular Photocatalyst for the Reduction of Au(III) to Au(I) and High-Turnover Generation of Gold Nanocrystals

Cédric Mongin,[†] Isabelle Pianet,[†] Gediminas Jonusauskas,[‡] Dario M. Bassani,*[,†] and Brigitte Bibal*[,†]

[†]Institut des Sciences Moléculaires, CNRS UMR 5255, Université de Bordeaux, 351, cours de la Libération, 33405 Talence, France

[‡]Laboratoire Ondes et Matière d'Aquitaine, UMR CNRS 5798, Université de Bordeaux, 351, cours de la Libération, 33405 Talence, France

ABSTRACT: We report a photocatalyst composed of a diphenylanthracene core appended with two lipophilic thioether side chains that binds gold(III) chloride. Upon excitation using visible light, the Au^{III} ions are smoothly reduced to Au^{I} which, in the presence of water, lead to the formation of crystalline gold nanoparticles of 20−50 nm diameter that are devoid of sulfur containing capping agents. Ultrafast transient absorption spectroscopy shows that the anthracene excited state is quenched with a rate $k = 3.5 \times 10^{10}$ s^{-1}, assigned to intramolecular energy transfer to the bound gold ions, which then oxidizes the solvent to produce an intermediate low valency gold(I) species. In the absence of water, the latter is stable and can be used as a homogeneous Au^{I} catalyst. When employed in a biphasic reactor, the photocatalyst shows average turnover numbers of 150 atoms of Au^{III} reduced to Au^{0} per molecule of photocatalyst.

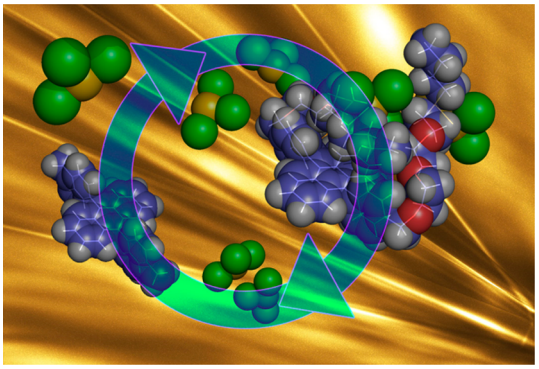

KEYWORDS: *gold, nanoparticle, photocatalyst, homogenous catalysis, diphenylanthracene*

1. INTRODUCTION

Supramolecular photocatalysts combine a molecular recognition motif with a photosensitizer designed to absorb light and promote a chemical transformation using a photoinduced electron or energy transfer process.[1,2] Several such systems have been explored toward cycloaddition reactions, isomerization, and free radical transformations.[3−5] In some cases, it has been possible to achieve turnovers greater than unity and mimic enzymatic behavior by combining hydrogen bonding interactions with photosensitizers for the oxidation of alcohols[6] or for catalyzing intramolecular cyclization.[7−10] The design of supramolecular photocatalysts has so far focused on the transformation of organic molecules as they can readily combine a reaction center and a molecular recognition motif within a single species. In contrast, the design of supramolecular photocatalysts for the generation of inorganic species remains undocumented despite the potential of using light for smoothly preparing metal based catalytic intermediates or metal frameworks[11] endowed with novel properties.

The photoinduced reduction of $AuCl_3$ by triplet benzophenone was recently investigated in detail by the group of Scaiano and shown to proceed via a diffusion limited photoinduced electron transfer to generate Au nanoparticles (AuNP) and benzophenone oxidation products.[12] We reasoned that a photosensitizer might be able to drive the photoreduction of a metal ion such as Au^{III} either by pumping electrons from the solvent to the gold ions, or by exciting the gold ions via an energy transfer mechanism. Such a system would be very useful for providing a photochemical route toward low valent Au species using long wavelength light that is not absorbed by common small organic molecules, as well as providing an example of the use of an organic photocatalyst for the generation of an inorganic material. Based on this, we designed a supramolecular photocatalyst containing a diphenylanthracene chromophore appended with two metal binding thioether side chains as such systems can promote strong interactions between the photoactive moiety and the metal ions.[13] The thioether side chains are very lipophilic and render the gold−photocatalyst assembly soluble in organic solvents, thus allowing its selective photoexcitation while preventing background irradiation of nonbound Au^{III} that remains in the aqueous phase. We show that the system can be readily steered toward either the production of a homogeneous Au^{I} catalyst that can be directly used in organic synthesis, or toward the formation of uncapped gold nanocrystals. The latter can be produced in large quantities through the use of a recirculating reactor in which the catalyst reaches up to 170 catalytic cycles. Such turnover numbers are unprecedented for a supramolecular photocatalyst and demonstrate that photocatalytic generation of an inorganic material by an organic catalyst can be highly efficient. The reaction mechanism was elucidated by a combination of ultrafast absorption spectroscopy, product analysis, and dynamic ^{1}H NMR spectroscopy.

Scheme 1. Chemical Structure of 1 and Proposed Structure of the 1·2AuCl$_3$ Complex Obtained by Complexation of Two Molecules of AuCl$_3$, and after Photoreduction to 1·2AuCl

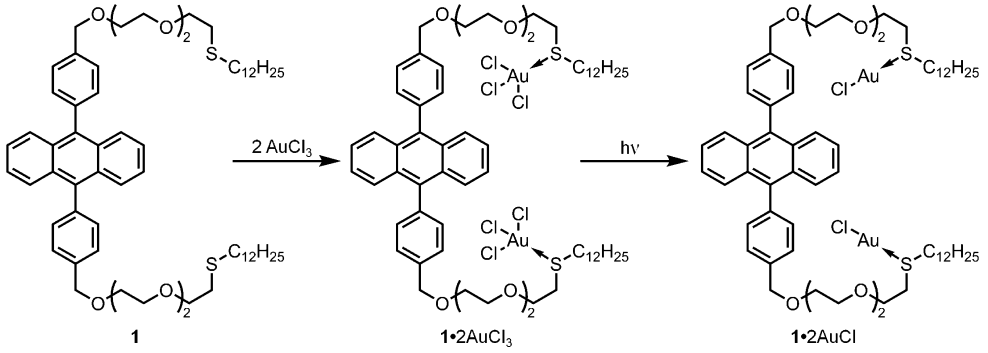

2. EXPERIMENTAL SECTION

2.1. General Protocols. Reaction quantum yield measurements were measured at low conversion using monochromatic radiation from a medium pressure Xe−Hg lamp equipped with a monochromator. The samples (aerated) possessed absorbance ≥2 at the excitation wavelength and were stirred throughout the irradiation. Ferrioxalate actinometry was used to determine the photon flux (using $\Phi(Fe^{III} \rightarrow Fe^{II}) = 1.20$ and 1.13 at 313 and 380 nm, respectively)[14] and the Au^{III} concentration was determined spectroscopically. Fluorescence quantum yields were determined by comparison to a secondary standard (quinine sulfate in 2 N H_2SO_4, $\Phi_F = 0.54$).[14]

2.2. Preparation of Gold(III) and Gold(I) Complexes. Complex **1**·2AuCl$_3$ was obtained by two methods that gave identical results: (i) dissolution of solid HAuCl$_4$ or KAuCl$_4$ into a solution of **1** (toluene or dichloromethane) or (ii) extraction of AuCl$_3$ from an aqueous solution of HAuCl$_4$ by a solution of **1** in toluene or dichloromethane. The binding of AuCl$_3$ by **1** was followed spectroscopically by monitoring the absorption of Au(III) at 330 nm, and the complexes were characterized using mass spectroscopy (FD^+). Complex **1**·2AuCl was obtained by irradiating a solution of **1**·2AuCl$_3$ in toluene (0.1−1 mM), at 20 °C, using a TLC lamp (365 nm, 6W) or LED (400 nm, 10W), for 15−30 min.

2.2. Preparation of AuNP. A solution of **1**·2AuCl$_3$ in dichloromethane or toluene (0.1 to 1 mM, 10 mL) was prepared in a centrifugation tube (50 mL). Water (10 mL) was added and the biphasic system was agitated on an orbital stirring table at 300 rpm while irradiated using a TLC lamp (365 nm, 6W) or a LED (400 nm, 10W) for 15 min. The reaction mixture was then centrifuged at 1500 rpm for 15 min and the aqueous phase, containing gold nanoparticles, was collected.

2.3. Photoreduction Reactor and Calculation of Turnover Number. To estimate the maximum number of turnover cycles that can be performed by **1**, the recirculating reactor described in Figure 9 was loaded with **1** (initial concentration = 15 μM, Vol = 40 mL) and an excess of HAuCl$_4$ (initial concentration = 6 mM, Vol = 50 mL). The absorption spectrum of the aqueous phase was monitored at t = 0 and 15 h (end of conversion) by withdrawing an aliquot (100 μL) and diluting it in 2 mL H_2O. Using the extinction coefficient of the HAuCl$_4$ solution at 290 nm, the concentration of Au^{III} remaining in solution can be determined. The turnover number is calculated in terms of moles of consumed Au^{III} ions per moles of **1** consumed.

3. RESULTS AND DISCUSSION

3.1. Synthesis and Characterization of Au Complex. The photocatalyst used in this study is easily prepared in three steps from commercially available reagents (72% overall yield). All spectroscopic analyses are consistent with the structures shown in Scheme 1. As expected for diphenylanthracene derivatives, **1** is highly fluorescent in nonpolar organic solvents (Φ_F = 0.96, τ = 7.5 ns in toluene, λ_{ex} = 365 nm), although photooxidation of the thioether groups occurs in solvents of moderate polarity via a known photoinduced electron transfer mechanism.[15,16]

The thioethers in **1** are designed to bind two AuCl$_3$ and maintain them in the vicinity of the anthracene chromophore. With this in mind, flexible ethylene glycol subunits were introduced in the linker to alleviate unfavorable gauche interaction associated with folding of the chain. To examine compound **1**'s ability to bind AuCl$_3$, a solution of **1** in dichloromethane or toluene was placed in contact with an aqueous solution of HAuCl$_4$ or with solid AuCl$_3$. Upon gentle shaking, the yellow color of the Au^{III} was transferred to the organic phase which became nonfluorescent. Complexation can be readily followed by UV−vis or emission spectroscopy (Figure 1). In all cases, whether by titration of **1** by the Au^{III} salt or by measuring the amount of Au^{III} salt lost from the aqueous phase upon incremental addition of **1**, the stoichiometry was found to be 1:2 (**1**: AuCl$_3$).

In agreement with the formation of a 1:2 complex, mass spectrometric analysis of the organic phase following extraction

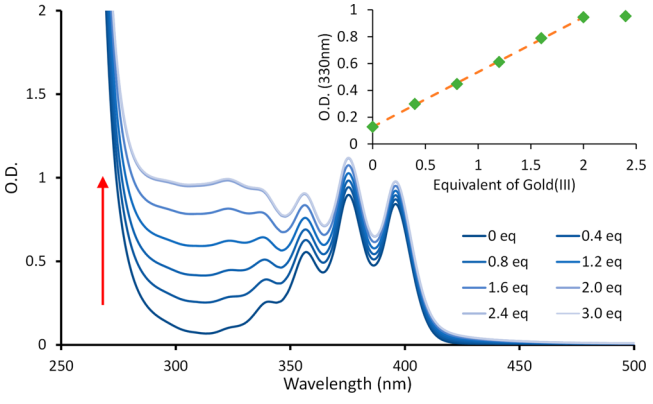

Figure 1. Variation of the absorbance of a solution of **1** (60.5 μM, CH_2Cl_2) upon addition of solid HAuCl$_4$. (inset) Variation of the OD at 330 nm, which reaches a maximum at 2 equiv of HAuCl$_4$.

of $AuCl_3$ by **1** evidenced the presence of a molecular ion with m/z = 1630 Da corresponding to a species with the formula **1**·2$AuCl_3$ (Figure 2A). Irradiation of anhydrous **1**·2$AuCl_3$ solutions in

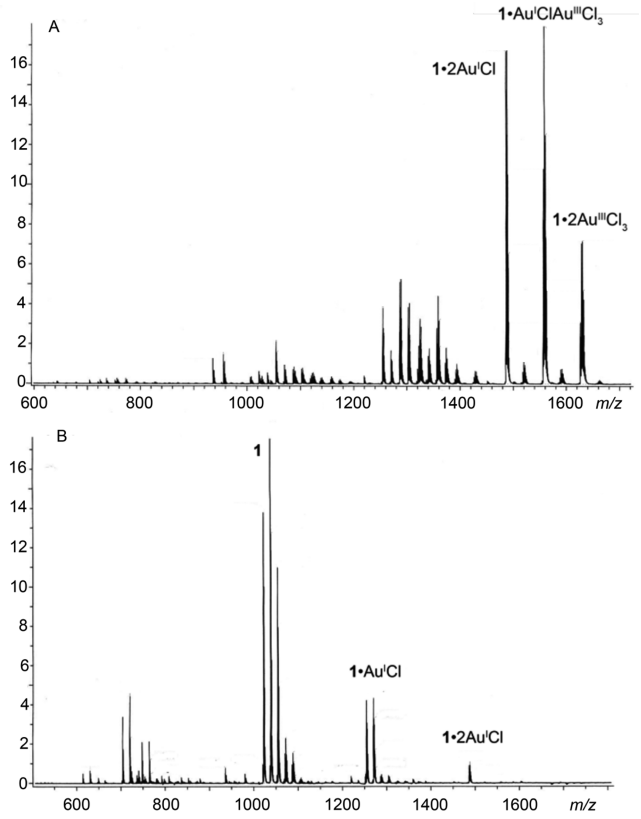

Figure 2. (A) Mass spectrum (FD+) of **1**·2$AuCl_3$ in toluene obtained by extraction of an aqueous solution of $HAuCl_4$. Partial reduction of the bound Au^{III} is assigned to exposure to ambient light during sample preparation. (B) Mass spectroscopic analysis (FD+) of the same solution following irradiation at 365 nm (15 min) shows free **1** along with **1** bound to 1 or 2 equiv of AuCl.

toluene or dichloromethane (aerated or Ar saturated) at 365 or 400 nm, where the diphenylanthracene chromophores absorbs, results in the rapid reduction of the Au^{III} into Au^{I}, as evidenced by the discoloration of the solution and by MS analysis of the photolyzed solution which now only shows signals corresponding to the dissociation of **1**·2$AuCl_3$ (Figure 2B).

The solid state structure of the **1**·2$AuCl_3$ complex is not currently known, as it is a waxy solid that is not amenable to X ray diffraction analysis. However, binding of $AuCl_3$ is likely to occur at the sulfur positions in **1** as generally observed for thioethers (Scheme 1).[17] Diffusion ordered NMR spectroscopy (DOSY)[18] was used to obtain information regarding the diffusion constant of **1** and the **1**·2$AuCl_3$ complex in dichloromethane (Figure 3). The latter gives a narrow distribution of diffusional rates centered around the value of 5.44×10^{-10} m^2/s, compared to a diffusion constant of 1.75×10^{-9} m^2/s for **1** under the same conditions. In the case of the **1**·2$AuCl_3$ complex, the observed diffusion constant corresponds to a calculated Stokes radius of R_S = 8.9 Å (V_S = 2950 Å^3), which is in good agreement with the solvent excluded volume calculated for a compact structure using a PM5 semiempirical model (3250 Å^3). The observation that the ^{1}H NMR spectrum of the **1**·2$AuCl_3$ complex is sharp, and that its diffusion coefficient is only reduced by one half with respect to **1** strongly argues against the formation of coordination polymer

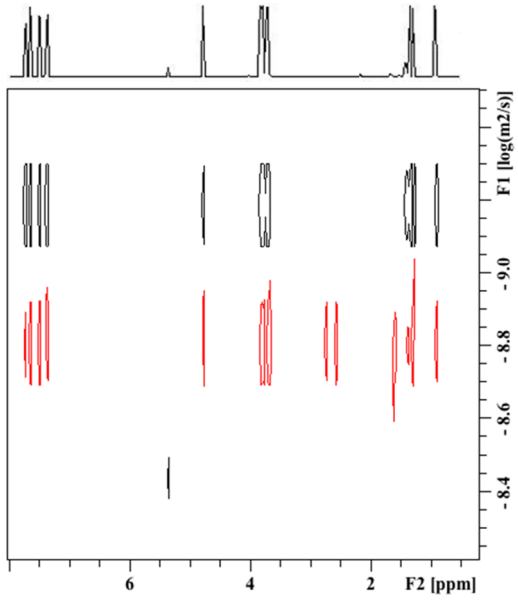

Figure 3. DOSY spectrum (600 MHz) of **1** (red) and **1**·2$AuCl_3$ complex (black) in dichloromethane d_2.

networks, which would be expected to exhibit broadened NMR signals and considerably reduced diffusional constants.

The formation of coordination polymers or aggregates would be expected to greatly influence the reduction of Au species by accelerating the formation of Au clusters and seeding.[19] To further verify that binding to $AuCl_3$ did not induce aggregation of the complex in solution, experiments using high field (800 MHz) and variable temperature ^{1}H NMR were undertaken. At room temperature, the ^{1}H NMR spectrum of the **1**·2$AuCl_3$ complex in CD_2Cl_2 is sharp, with the exception of the aromatic protons of the diphenylanthracene core which are somewhat broadened (see Figure 4A and B). No broadening of the dodecyl or ethylene glycol chains is observed, suggesting that the complex is not aggregated in solution and that the aromatic core experiences slow interconversion between different environments. Hindered rotation of the diphenylanthracene moiety in **1** would be expected upon complexation of Au^{III} if the complex adopts a compact conformation as suggested by the results from DOSY. In agreement with this, we find that these signals sharpen upon lowering the temperature to 203 K (Figure 4C). From the coalescence temperature of the aromatic protons at 7.4 ppm, an activation barrier for equilibration of ca. 60 kJ/mol is calculated. This behavior is contrary to that expected for aggregation, which is instead favored at low temperatures and generally induces increased broadening of NMR signals.

3.2. Photoreduction of Au^{III} and Catalytic Behavior of Au^{I} Complex. As mentioned above, irradiation of the **1**·2$AuCl_3$ complex in toluene or dichloromethane ($\lambda \geq 365$ nm) in the absence of water rapidly leads to the formation of AuCl species as expected for the photoreduction of the $AuCl_3$ salt. The efficiency of the reduction process can be monitored from the disappearance of the absorption band associated with Au^{III} bound to **1** upon selective irradiation of the anthracene chromophore. Irradiation at 380 nm of aerated toluene or dichloromethane solutions of **1**·2$AuCl_3$ led to the rapid disappearance of the absorption band of Au^{III} with quantum yields of 0.07 and 0.06, respectively. Because Au^{II} salts possess similar electronic transitions as Au^{III} salts, we believe that these values correspond to the formation of Au^{I} species,

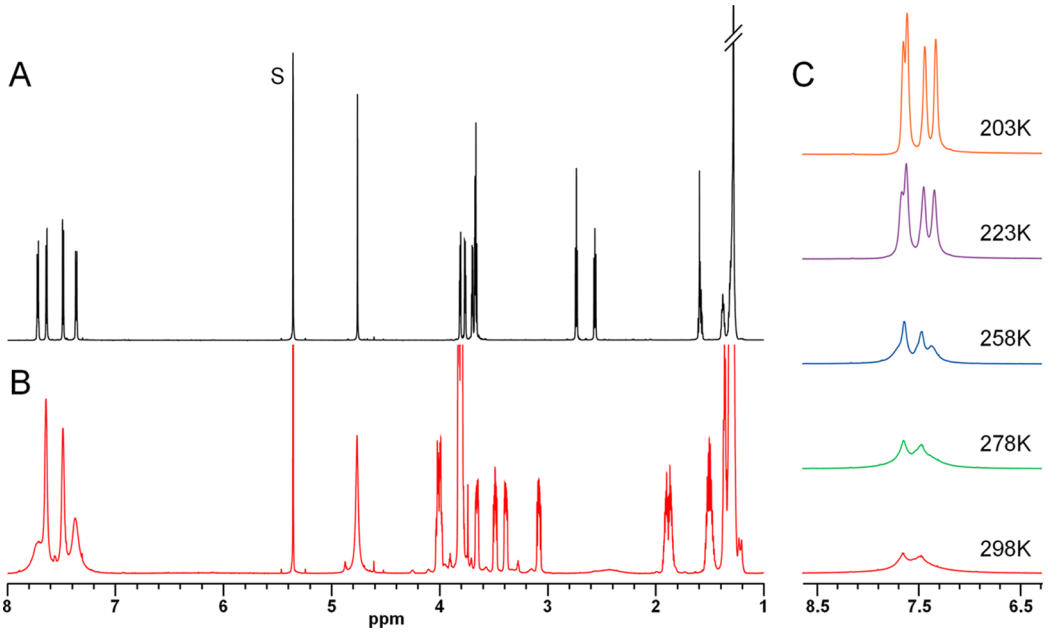

Figure 4. High field ^{1}H NMR (800 MHz, CD_2Cl_2) of **1** (A) and **1**·2$AuCl_3$. (B). The latter exhibits broadening of the signals of the aromatic protons, but not of the signals associated with the alkyl or ethylene glycol chains. This is interpreted as resulting from slow conformational interconversion of the anthracene moiety upon formation of the Au complex in agreement with VT NMR (600 MHz, CD_2Cl_2) which shows sharpening of the signals at low temperature C.

which are transparent in the visible and near UV region of the spectrum.[20] In this case, the observed quantum yields represent the overall reduction process of Au^{III} to Au^{I}, which would be two consecutive reduction steps. Thus, assuming that each of the two photoreduction steps leading to Au^{I} from Au^{III} occurs with similar efficiency, the overall quantum efficiency of each photoreduction process would be 0.26. This indicates that the sequential energy transfer/solvent oxidation process is efficient and comparable to that observed by reductive photoinduced electron transfer to Au^{III} from an excited donor.[12] Energy wasting processes, possibly through spin exchange quenching of the anthracene excited state and vibronic relaxation, therefore amount to a quantum yield of 0.74.

The photolyzed solution can be directly used to catalyze organic reactions promoted by Au^{I}. To demonstrate this, we investigated the intramolecular ring closure of *t* butyl propargylamide using photolyzed and nonphotolyzed solutions of **1**·2$AuCl_3$. It is known that the reaction is catalyzed by Au^{III} species to form the corresponding oxazole, whereas the use of an Au^{I} catalyst leads to the formation of the methylene dihydrooxazole.[21] As expected from the proposed photoreduction of Au^{III} to Au^{I}, the use of the irradiated **1**·2$AuCl_3$ solution led to the rapid and exclusive formation of the dihydrooxazole, whereas use of nonirradiated **1**·2$AuCl_3$ complex led to formation of the oxazole (Scheme 2). Thus, the supramolecular complex behaves as a light sensitive catalyst in which it is possible to control the nature of the catalytic species (Au^{I} or Au^{III}) simply by irradiation with visible light.

Scheme 2. Catalytic Activity of Homogeneous 1·2$AuCl_3$ and 1·2AuCl Formed by Irradiation on the Intramolecular Ring Closure of *t* Butyl Propargylamide

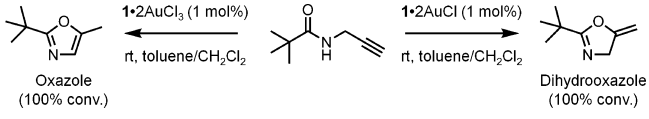

3.3. Photogeneration of Au Nanocrystals. In the absence of water, the **1**·2AuCl complex is relatively stable and undergoes slow dismutation over several days to form Au^0 and $AuCl_3$. In contrast, the presence of water promotes the formation of gold nanoparticles (AuNP), which is complete in 45−60 min in water/toluene or occurs during irradiation if water/dichloromethane is used as a reaction medium. The appearance of a ruby red coloration of the aqueous phase (λ_{max} = 535 nm) observed is typical of the absorption from the plasmon resonance of AuNP that are ca. 30 nm in size.[22,23] Transmission electron microscopy (TEM) images of the particles suspended in the aqueous phase are shown in Figure 5.

They unambiguously identify the nanoparticles as crystalline AuNP of dimensions that are between 20 and 50 nm. Further inspection shows that they are formed by the agglomeration along crystal growth axes of smaller (ca. 5 nm) AuNP that are also crystalline.

The process leading to the formation of AuNP is broadly similar to that previously observed for the photoreduction of aqueous solutions of Au complexes.[24−26] However, we observe that in this case the Au^0 atoms formed undergo nucleation and eventually migrate to the aqueous phase due to the hydrophilic nature of pristine gold,[27] thereby releasing the photocatalyst which remains in the organic phase. In support of this, X ray photoelectron spectroscopy (XPS) analysis of the AuNP reveals the presence of chlorine atoms along with carbon and oxygen, whereas the amount of sulfur atoms is below the detection limit (Figures 6). This result shows that **1** is not extracted into the aqueous phase along with the nanoparticles, which are instead stabilized by chloride anions and traces of organic molecules. The XPS analysis also revealed the presence of cationic Au species, which may also contribute to the stabilization

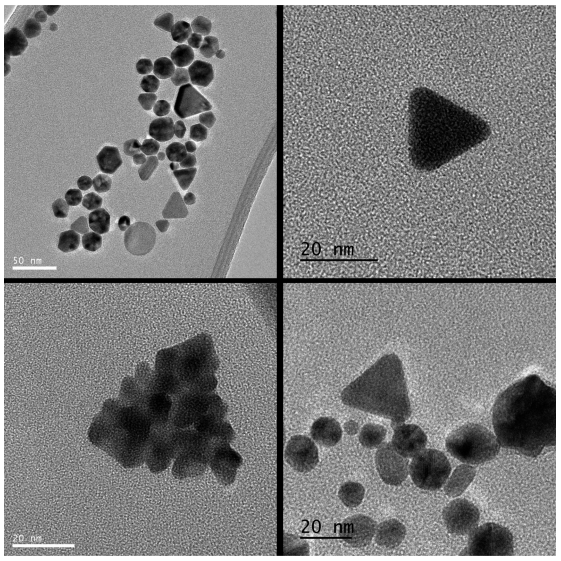

Figure 5. Transmission electron microscopy images of AuNP obtained by irradiation of the **1**·2$AuCl_3$ complex in toluene. The particles were prepared as described in the Experimental Section and deposited from the aqueous phase without further purification. In some cases (bottom left), the agglomeration of smaller crystalline particles and subsequent reorganization of the Au atoms can be observed.

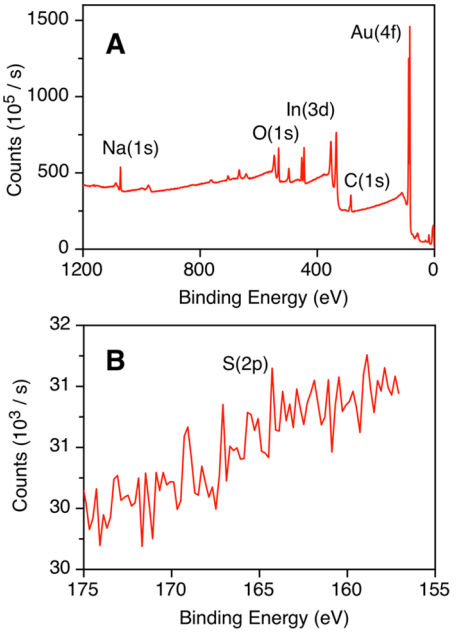

Figure 6. X ray photoelectron spectroscopy of AuNP obtained from irradiation of a toluene solution of **1**·2$AuCl_3$ deposited on an In substrate (A). The AuNP thus deposited were analyzed without washing or further purification. (B) Close up on the region where the signal for the S(2p) is expected (168.91 eV). Its absence confirms that neither **1** nor other sulfur containing fragments are extracted along with the AuNP.

of the AuNP and provide further opportunities for applications in catalysis.[28]

3.4. Mechanistic Investigation. Several pathways have been reported for the photoreduction of Au^{III} salts into AuNP, the most common of which being the use of pulse radiolysis or photoinduced fragmentation of a suitable precursor to generate a chemical reductant.[29,30] Direct irradiation of Au^{III} in the presence of ethylene glycol and a capping agent using broad wavelength UV light (250−400 nm) yields small (7 nm diameter) spherical AuNP through a mechanism involving glycol oxidation.[31] Uncapped AuNP can be obtained by reduction of $HAuCl_4$ by photogenerated ketyl radicals in water,[24] direct excitation of $AuCl_4^-$ in the presence of a reductant,[25] or via an electron transfer process from excited benzophenone.[12] However, all of these mechanisms result in the loss of the absorbing chromophore, which therefore does not exhibit catalytic activity. In contrast, we find that when toluene is used as the organic phase, there is no degradation of **1** and that the toluene solution of **1** can be isolated and reused to prepare another batch of AuNP. This cycle was repeated five times with no apparent loss of efficiency, confirming that **1** acts as a photocatalyst in contrast to previously reported photoreductants.

The mechanism by which $AuCl_3$ is reduced to Au^I or to Au^0 involves initial excitation of the diphenyanthracene chromo phore as this absorbs the majority of the incident radiation at $\lambda_{irr} \geq 365$ nm. Oxidative electron transfer quenching of the diphenylanthracene excited state by $AuCl_3$ would be expected to proceed through a single electron transfer to generate $Au^{II}Cl_2$ and is calculated to be thermodynamically favorable by $\Delta_{ET}G^0 = -0.5$ eV using eq 1,[32]

$$\Delta_{ET}G^{\circ} = N_A\{e[E^0(D^{+\bullet}/D) - E^0(A/A^{-\bullet})] + w(D^{+\bullet}A^{-\bullet})\} - \Delta E_{00} \quad (1)$$

where N_A is the Avrogado constant, e is the elementary charge, ΔE_{00} is the energy level of the singlet excited state of **1** (3.08 eV), and $E_0(D^{+\bullet}/D)$ and $E_0(A^{-\bullet}/A)$ refer to the oxidation and reduction potential of **1** (+1.46 V vs V_{NHE}) and $Au^{III}Cl_3$, respectively. The reduction potential of the Au^{III}/Au^I couple was bracketed between +0.35 and +0.71 V by Scaiano and co workers,[12] and a value of +0.6 V vs V_{NHE} as estimated by Gachard et al. from pulse radiolysis experiments[33] was used in the calculation. The Coulombic term was calculated according to $w(D^{+\bullet}A^{-\bullet}) = 2e^2/(4\pi\varepsilon_0\varepsilon_r a)$, where ε_0 and ε_r are the vacuum and relative electric permittivity, respectively, and a is the separation between $D^{+\bullet}$ and $A^{-\bullet}$ (0.7 nm).

Photoinduced electron transfer in **1**·2$AuCl_3$ would be expected to be fast as it is intramolecular and not limited by the diffusion of the reactants. Femto second time resolved transient absorption spectroscopy was therefore used to identify the initially formed excited state as well as the primary photoinduced processes upon light absorption. In the case of electron transfer quenching, the ensuing diphenylanthracene radical cation possesses a characteristic spectral signature at 500−600 nm that is easily identified.[34] Upon pulsed excitation (λ_{ex} = 380 nm, 40 fs), the absorption spectrum of the S_1 state of the diphenylanthracene chromophore is clearly visible (λ_{max} = 560 nm, Figure 7), thereby excluding direct population of the anthracene triplet state owing to strong spin−orbit coupling induced by the Au atoms. The anthracene S_1 signal decreases rapidly with a time constant of 27 ps (in either toluene or dichloromethane), from which a rate constant for intramolecular quenching of the singlet excited state of **1** by the bound gold ions $k_q = 3.7 \times 10^{10}$ s^{-1} can be determined. However, no signal corresponding to the absorption of the radical cation of **1** or of the diphenylanthracene T_1 state can be detected, and the repopulation of the ground state was found to occur on the same time scale as the depopulation of the S_1 excited state.[35] This implies that either the ensuing reaction of the diphenylan

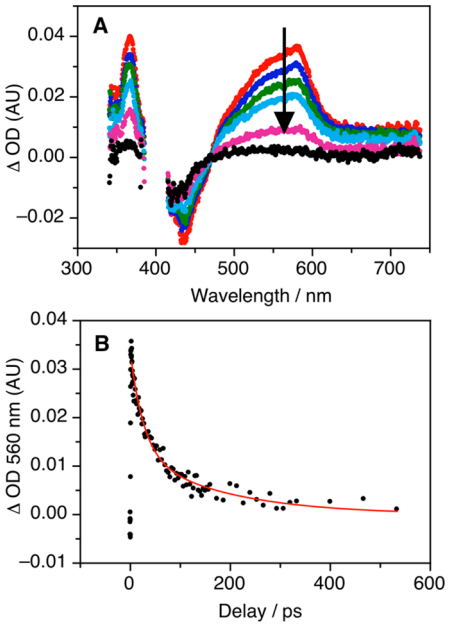

Figure 7. (A) Transient absorption spectra at various delays after excitation (λ_{ex} = 380 nm, 40 fs pulses, delays from top to bottom: 2, 5, 12, 20, 80, 300 ps) of a solution of **1**·2$AuCl_3$ complex in toluene and (B) decay of the transient signal observed at 560 nm, corresponding to the S_1 of the diphenylanthracene chromophore in **1**. The solid line represents the best fit to a decay with $k = 3.7 \times 10^{10}$ s^{-1}.

thracene radical cation occurs with a rate $\geq 3.7 \times 10^{10}$ s^{-1} or, more likely, that the quenching mechanism occurs via an energy transfer pathway as this would directly repopulate S_0 without any intermediate states. This latter possibility is intriguing as one might expect energy transfer from the diphenylanthracene singlet excited state to be spin forbidden in view of the predominantly triplet character of the Au^{III} excited state, and the process is likely facilitated by strong spin−orbit coupling or may proceed through a spin exchange mechanism.[36]

Intramolecular energy transfer from the excited diphenylan thracene chromophore to Au^{III} could occur via a spin exchange processor via dipole−dipole interactions (FRET mechanism). The former requires orbital overlap between the donor and acceptor which is not apparent from the ^{1}H NMR or electronic absorption spectrum of the complex. In the case of FRET, the distance separating the donor−acceptor pair can be calculated from the observed energy transfer rate and the overlap integral between the emission spectrum of the donor and the absorption spectrum of the acceptor using eq 2,[37]

$$k_{EnT} = \frac{1}{\tau_D}\left(\frac{R_0}{r}\right)^6 \quad (2)$$

where τ_D is the lifetime of the excited donor and R_0 is the Förster radius (calculated from the spectral overlap to be 2.3). From eq 2, an average Au− anthracene distance of 9 Å is calculated for quenching in the **1**· 2$AuCl_3$ complex, which is consistent with an intramolecular energy transfer process.[38]

Comparison of dichloromethane and toluene as an organic medium reveals important differences in behavior. When dichloromethane is used, MS and NMR analysis of the organic phase after formation of the AuNP show that **1** has decomposed, principally by cleavage of the chains in the benzylic position and α to the thioethers. In contrast, when toluene is used as an organic phase, **1** does not decompose and the presence of toluene byproducts (benzyl chloride, benzaldehyde, chloroto luene) is detected instead. These may be formed through a mechanism involving oxidation of toluene by photoexcited Au^{III} or through the release of chloride radicals from the **1**·2$AuCl_3$ complex analogously to the photoejection of Cl· from $AuCl_4^-$ as described by McGillivray et al.[25]

From the experimental observations, a reaction mechanism can be proposed for the photoreduction of Au^{III} into Au^I, which in the presence of water continues to the reduction of Au^I into AuNP (Figure 8). Catalyst **1** binds two $AuCl_3$ molecules to form a **1**·2$AuCl_3$ complex that is soluble in the organic phase. Upon excitation at 400 nm, the anthracene chromophore is excited preferentially and ultrafast energy transfer populates the Au^{III}* excited state which is a strong photooxidant.[39,40] If the reaction is conducted in toluene, the excited Au^{III} complex oxidizes the solvent to produce Au^{II} ions and toluene oxidation byproducts. If toluene is replaced by dichloromethane, then the excited Au^{III} complex oxidizes **1**, eventually leading to its decomposition. It is commonly assumed that Au^{II} species formed during the reduction of Au^{III} ions undergo dismutation to form Au^I and Au^{III}.[29] This is indeed observed if the irradiation is stopped after 1−2 min, but the process is relatively slow as the concentrations involved are low (several hours). This is not entirely compatible with the rapid transformation of Au^{III} that is observed upon continued irradiation and it is possible that a light induced process for the consumption of Au^{II} is also operating in competition with dismutation of Au^{II}. Because it is known that

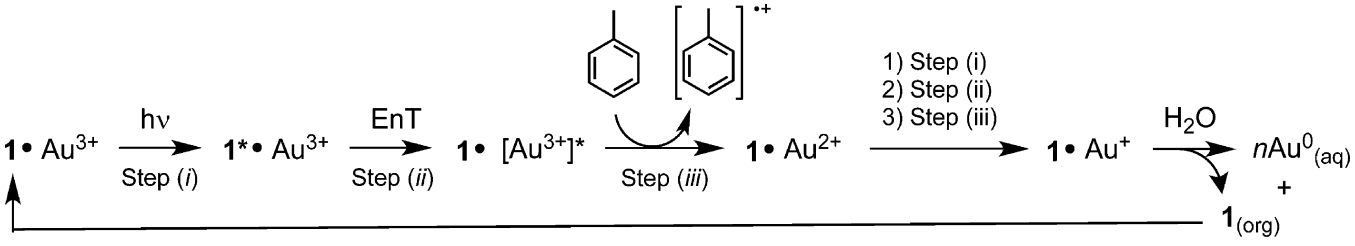

Figure 8. Proposed catalytic cycle accounting for the reduction of $AuCl_3$ in toluene. Compound **1** binds two $AuCl_3$ molecules and draws them into the organic phase, where they are irradiated (step i, 365 nm (TLC lamp) or 405 nm (LED)). Excitation of the diphenylanthracene chromophore is followed by ultrafast energy transfer to the $AuCl_3$ center (step ii), which oxidized the solvent (toluene) and is consequently reduced. The entire process occurs twice per bound Au^{III} atom to produce Au^I which then forms Au^0 in the presence of water. Alternatively, it is possible that the Au^{II} produced undergoes dismutation to form Au^{III} and Au^I, and the process is repeated (not shown, see text). In the presence of water, nucleation of the Au^0 atoms leads to the formation of AuNP which migrate to the aqueous phase and release **1** into organic phase to continue the reduction cycle.

Au^{II} species absorb more intensely and at longer wavelengths than the corresponding Au^{III} complexes,[20] it is possible that energy transfer to the Au^{II} complex from the diphenylanthracene S_1 state is as fast or faster than energy transfer to the Au^{III} species. The excited Au^{II}* ion would once again oxidize the solvent to generate Au^{I}. The latter does not absorb in the visible range,[20] thereby stopping the energy transfer quenching of the S_1(**1**) excited state.

3.5. Catalytic Turnover. In order to calculate the maximum turnover cycles of **1** in toluene, we constructed a recirculating reactor that allows the selective excitation of the organic phase while protecting the aqueous phase from light to avoid possible background photoreduction of excess Au^{III} (Figure 9). The

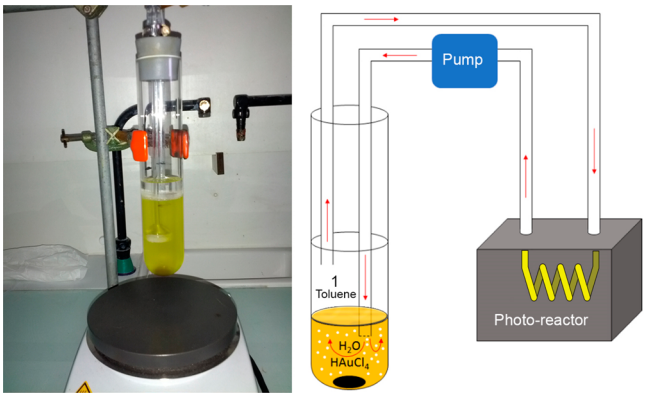

Figure 9. Recirculating reactor constructed to determine the maximum turnover cycles attainable by **1**. The biphasic reactor draws the toluene solution of the **1**·2$AuCl_3$ complex from the supernatant, which is then sent to a photoreactor enclosure composed of glass tubing that is irradiated by two 400 nm 10 W LED sources. The irradiated solution is then pumped back into the reactor through a glass frit located in the aqueous subphase in which an excess of $HAuCl_4$ is present. The amount of Au^{III} present in the aqueous phase is determined spectroscopically at various intervals.

reactor is composed of an extractor in which the catalyst in the toluene organic phase is exposed to a large excess of $HAuCl_4$ contained in the aqueous phase. The supernatant organic solution is pumped through a glass tube that is exposed to two 10 W 400 nm LED sources and then circulated back into the aqueous subphase through a fritted glass membrane. The pumping rate was adjusted to allow a 10−15 min exposure to the irradiation, and it was immediately apparent that the solution leading into the photochemical reactor was nonfluorescent, whereas that exiting the photochemical reactor was highly fluorescent. The amount of $Au^{III}Cl_4^-$ remaining in the aqueous phase was analyzed by UV−vis absorption at various times. Upon operation, the aqueous phase became red and a reddish precipitate formed on the fritted glass as expected for the formation of AuNP. The experiment was repeated 5 times, yielding an average turnover number (TON) of Au^{III} atoms reduced per molecule of **1** consumed of TON = 146 (σ = 20, TON_{max} = 174, TON_{min} = 120, see Table 1). Continued irradiation after all **1** had been consumed did not lead to further reduction of Au^{III}. It is likely that optimization of the experimental conditions could further increase the turnover of the catalyst, but it should be noted that this figure is already significant in comparison with previous reports of supra molecular photocatalysts.

4. CONCLUSIONS

Photoinduced processes are inherently quantized and, unlike chemical reduction of Au^{III}, photoreduction using **1** as a photocatalyst allows the straightforward preparation of low valent Au^{I} salts that can be of interest for applications in catalysis of organic reactions. We have shown that bound Au^{III} is efficiently and selectively reduced to Au^{I} using long wavelength irradiation ($\lambda \geq 380$ nm) and that the resulting Au^{I} complex is catalytically active toward a prototypical organic transformation. In this respect, the system is very different from those previously reported that make use of a photogenerated reductant and which invariably lead to the production of AuNP. By avoiding the presence of water, it is possible to steer the photoreduction toward the exclusive generation of Au^{I} species. In this case, the supramolecular complex becomes a light sensitive catalyst that makes it possible to control the nature of the catalytic species (Au^{I} or Au^{III}) by irradiation with visible light. The use of energy transfer from an organic sensitizer allows longer wavelength irradiation to be used, which is desirable to avoid direct excitation of the substrates or products that are present in the reaction mixture.

The synthesis of uncapped crystalline AuNP is interesting for their development for applications in medicine,[41] plasmonics, and catalysis.[42,43] It has been noted that the presence of cationic Au species,[28] or that of organic stabilizers,[44] can profoundly influence their catalytic activity. Although several routes for the photochemical preparation of AuNP are already known,[12,24,25,31,45−51] it remains remarkable that this can be efficiently accomplished using an organic photocatalyst and this is an important milestone in the development of supramolecular systems for materials synthesis. Furthermore, it has been recently shown that the presence of organic stabilizers influences the catalytic activities of AuNP and there is therefore interest in the development of facile approaches to the preparation of uncapped AuNP. We are currently exploring this approach toward other transition metal ions possessing low lying excited states by adapting the energy level of the photosensitizer and the nature of the chelating sites.

Table 1. Initial and Final Au^{III} Concentrations from Five Runs of Au^{III} Reduction Using the Recirculating Reactor Shown in Figure 9[a]

run	1		2		3		4		5	
t (h)	0	15	0	15	0	15	0	15	0	15
OD (287 nm)	0.797	0.592	0.821	0.567	0.788	0.521	0.745	0.447	0.787	0.581
$[Au^{III}]^b$ (mM)	5.58	3.98	5.75	3.97	5.52	3.65	5.21	3.13	5.51	4.06
TON	133		148		156		174		121	

[a] V_{aq} = 50 mL, [**1**] = 15 μM, V_{org} = 40 mL. [b] Determined using $\varepsilon(HAuCl_4, 290\ nm) = 3150\ M^{-1}\cdot cm^{-1}$.

AUTHOR INFORMATION

Corresponding Authors

*Fax: (+33) 5 4000 6158. Tel.: +33 5 4000 2827. E mail: d. bassani@ism.u bordeaux1.fr (D.M.B.).

*Tel.: +33 5 4000 3364. E mail: b.bibal@ism.u bordeaux1.fr (B.B.).

Notes

The authors declare no competing financial interest.

ACKNOWLEDGMENTS

The authors thank C. Absalon and P. Castel for help with the mass spectrometry analyses and A. Grélard for the high field NMR experiments. Financial support from the University of Bordeaux, the Conseil Regional Aquitain, and CNRS is gratefully acknowledged.

REFERENCES

(1) Svoboda, J.; König, B. *Chem. Rev.* **2006**, *106*, 5413−5430.

(2) Bibal, B.; Mongin, C.; Bassani, D. M. *Chem. Soc. Rev.* **2014**, *43*, 4179−4198.

(3) Zeitler, K. *Angew. Chem., Int. Ed.* **2009**, *48*, 9785−9789.

(4) Neumann, M.; Füldner, S.; König, B.; Zeitler, K. *Angew. Chem., Int. Ed.* **2011**, *50*, 951−954.

(5) Bassani, D. M.; Sallenave, X.; Darcos, V.; Desvergne, J. P. *Chem. Commun.* **2001**, 1446−1447.

(6) Cibulka, R.; Vasold, R.; König, B. *Chem.—Eur. J.* **2004**, *10*, 6223−6231.

(7) Bauer, A.; Westkamper, F.; Grimme, S.; Bach, T. *Nature* **2005**, *436*, 1139−1140.

(8) Müller, C.; Bauer, A.; Maturi, M. M.; Cuquerella, M. C.; Miranda, M. A.; Bach, T. *J. Am. Chem. Soc.* **2011**, *133*, 16689−16697.

(9) Austin, K. A. B.; Herdtweck, E.; Bach, T. *Angew. Chem., Int. Ed.* **2011**, *50*, 8416−8419.

(10) Müller, C.; Bauer, A.; Bach, T. *Angew. Chem., Int. Ed.* **2009**, *48*, 6640−6642.

(11) Jiang, X. F.; Hau, F. K. W.; Sun, Q. F.; Yu, S. Y.; Yam, V. W. W. *J. Am. Chem. Soc.* **2014**, *136*, 10921−10929.

(12) McTiernan, C. D.; Alarcon, E. I.; Hallett Tapley, G. L.; Murillo Lopez, J.; Arratia Perez, R.; Netto Ferreira, J. C.; Scaiano, J. C. *Photochem. Photobiol. Sci.* **2014**, *13*, 149−153.

(13) Witulski, B.; Zimmermann, Y.; Darcos, V.; Desvergne, J. P.; Bassani, D. M.; Bouas Laurent, H. *Tetrahedron Lett.* **1998**, *39*, 4807−4808.

(14) Montalti, M.; Credi, A.; Prodi, L.; Gandolfi, T. *Handbook of Photochemistry*, Third ed.; Taylor & Francis, 2006.

(15) Bonesi, S. M.; Manet, I.; Freccero, M.; Fagnoni, M.; Albini, A. *Chem.—Eur. J.* **2006**, *12*, 4844−4857.

(16) Latour, V.; Pigot, T.; Simon, M.; Cardy, H.; Lacombe, S. *Photochem. Photobiol. Sci.* **2005**, *4*, 221−229.

(17) Murray, S. G.; Hartley, F. R. *Chem. Rev.* **1981**, *81*, 365−414.

(18) Cohen, Y.; Avram, L.; Frish, L. *Angew. Chem., Int. Ed.* **2005**, *44*, 520−554.

(19) Jana, N. R.; Gearheart, L.; Murphy, C. J. *Chem. Mater.* **2001**, *13*, 2313−2322.

(20) Dey, G. R.; El Omar, A. K.; Jacob, J. A.; Mostafavi, M.; Belloni, J. *J. Phys. Chem. A* **2011**, *115*, 383−391.

(21) Weyrauch, J. P.; Hashmi, A. S. K.; Schuster, A.; Hengst, T.; Schetter, S.; Littmann, A.; Rudolph, M.; Hamzic, M.; Visus, J.; Rominger, F.; Frey, W.; Bats, J. W. *Chem.—Eur. J.* **2010**, *16*, 956−963.

(22) Amendola, V.; Meneghetti, M. *J. Phys. Chem. C* **2009**, *113*, 4277−4285.

(23) Haiss, W.; Thanh, N. T. K.; Aveyard, J.; Fernig, D. G. *Anal. Chem.* **2007**, *79*, 4215−4221.

(24) McGilvray, K. L.; Decan, M. R.; Wang, D.; Scaiano, J. C. *J. Am. Chem. Soc.* **2006**, *128*, 15980−15981.

(25) McGilvray, K. L.; Granger, J.; Correia, M.; Banks, J. T.; Scaiano, J. C. *Phys. Chem. Chem. Phys.* **2011**, *13*, 11914−11918.

(26) Teets, T. S.; Nocera, D. G. *J. Am. Chem. Soc.* **2009**, *131*, 7411−7420.

(27) Smith, T. *J. Colloid Interface Sci.* **1980**, *75*, 51−55.

(28) Fu, L.; Wu, N. Q.; Yang, J. H.; Qu, F.; Johnson, D. L.; Kung, M. C.; Kung, H. H.; Dravid, V. P. *J. Phys. Chem. B* **2005**, *109*, 3704−3706.

(29) Zhao, P.; Li, N.; Astruc, D. *Coord. Chem. Rev.* **2013**, *257*, 638−665.

(30) Scaiano, J. C.; Billone, P.; Gonzalez, C. M.; Marett, L.; Marin, M. L.; McGilvray, K. L.; Yuan, N. *Pure Appl. Chem.* **2009**, *81*, 635−647.

(31) Eustis, S.; Hsu, H. Y.; El Sayed, M. A. *J. Phys. Chem. B* **2005**, *109*, 4811−4815.

(32) Braslavsky, S. E. *Pure Appl. Chem.* **2009**, *79*, 293−465.

(33) Gachard, E.; Remita, H.; Khatouri, J.; Keita, B.; Nadjo, L.; Belloni, J. *New J. Chem.* **1998**, *22*, 1257−1265.

(34) Shida, T. *Electronic Absorption Spectra of Radical Ions*; Physical Sciences Data; Elsevier: Amsterdam, 1988; Vol. *34*.

(35) A ground state recovery rate of 1.7×10^{10} s^{-1} is found. The recovery of the ground state absorption incudes contribution form vibronic relaxation and overlaps with stimulated emission and fluorescence, which makes accurate signal analysis difficult.

(36) Che, C. M.; Lai, S. W. In *Gold Chemistry. Applications and Future Directions in the Life Sciences*; Mohr, F., Ed.; Wiley VCH Verlag GmbH & Co. KGaA, 2009; p 249−281.

(37) Förster, T. *Ann. Phys.* **1948**, *437*, 55−75.

(38) From the excited state lifetime of **1**, the quantum yield for intramolecular energy transfer can be estimated to be > 99%.

(39) Chan, C. W.; Wong, W. T.; Che, C. M. *Inorg. Chem.* **1994**, *33*, 1266−1272.

(40) To, W. P.; Tong, G. S. M.; Lu, W.; Ma, C.; Liu, J.; Chow, A. L. F.; Che, C. M. *Angew. Chem., Int. Ed.* **2012**, *51*, 2654−2657.

(41) Dreaden, E. C.; Mackey, M. A.; Huang, X.; Kang, B.; El Sayed, M. A. *Chem. Soc. Rev.* **2011**, *40*, 3391−3404.

(42) Daniel, M. C.; Astruc, D. *Chem. Rev.* **2004**, *104*, 293−346.

(43) Sanchez, A.; Abbet, S.; Heiz, U.; Schneider, W. D.; Häkkinen, H.; Barnett, R. N.; Landman, U. *J. Phys. Chem. A* **1999**, *103*, 9573−9578.

(44) Zhong, R. Y.; Sun, K. Q.; Hong, Y. C.; Xu, B. Q. *ACS Catal.* **2014**, 3982−3993.

(45) Kajimoto, S.; Shirasawa, D.; Horimoto, N. N.; Fukumura, H. *Langmuir* **2013**, *29*, 5889−5895.

(46) Amendola, V.; Meneghetti, M. *Phys. Chem. Chem. Phys.* **2009**, *11*, 3805−3821.

(47) Dong, S.; Tang, C.; Zhou, H.; Zhao, H. *Gold Bulletin* **2004**, *37*, 187−195.

(48) Giorgetti, E.; Muniz Miranda, M.; Marsili, P.; Scarpellini, D.; Giammanco, F. *J. Nanopart. Res.* **2012**, *14*, 1−13.

(49) Henglein, A.; Meisel, D. *Langmuir* **1998**, *14*, 7392−7396.

(50) Kabashin, A. V.; Meunier, M. *J. Appl. Phys.* **2003**, *94*, 7941−7943.

(51) Storti, B.; Elisei, F.; Abbruzzetti, S.; Viappiani, C.; Latterini, L. *J. Phys. Chem. C* **2009**, *113*, 7516−7521.